JPE 15-5-22

http://dx.doi.org/10.6113/JPE.2015.15.5.1358
ISSN(Print): 1598-2092 / ISSN(Online): 2093-4718

Super-Twisting Sliding Mode Control Design for Cascaded Control System of PMSG Wind Turbine

Dinh Hieu Phan[†,*] and ShouDao Huang[**]

[†,**]College of Electrical and Information Engineering, Hunan University, Hunan, China
[*]Faculty of Mechanical Engineering, Hanoi University of Industry, Hanoi City, Vietnam

Abstract

This study focuses on an advanced second-order sliding mode control strategy for a variable speed wind turbine based on a permanent magnet synchronous generator to maximize wind power extraction while simultaneously reducing the mechanical stress effect. The control design based on a modified version of the super-twisting algorithm with variable gains can be applied to the cascaded system scheme comprising the current control loop and speed control loop. The proposed control inheriting the well-known robustness of the sliding technique successfully deals with the problems of essential nonlinearity of wind turbine systems, the effects of disturbance regarding variation on the parameters, and the random nature of wind speed. In addition, the advantages of the adaptive gains and the smoothness of the control action strongly reduce the chatter signals of wind turbine systems. Finally, with comparison with the traditional super-twisting algorithm, the performance of the system is verified through simulation results under wind speed turbulence and parameter variations.

Key words: Maximum power point tracking, Permanent magnet synchronous generator, Sliding mode control, Super-twisting algorithm, Variable wind turbine

I. INTRODUCTION

The wind turbine is one of the fastest growing renewable energy technologies available today. The total globally installed wind capacity has been growing significantly during the past decade, reaching 318GW at the end of 2013. This is an increase of 12.5% compared with the 2012 market [1]. Among currently available wind energy conversion systems (WECSs), variable speed wind turbines are preferable to fixed speed ones because of their ability to maximize power extraction energy and increase efficiency [2]. In variable speed wind turbines, wind turbine based on permanent magnet synchronous generator (PMSG) offers several benefits in the wind power applications, such as their high power density, high efficiency, more reliability, and easy maintenance. These features make it an attractive choice in the wind turbine systems [3], [4]. It is widely known that the main control objective for the wind turbines in the low speed region is power efficiency maximization.

To achieve this goal, the turbine tip speed ratio should be maintained at its optimum value despite wind speed variation. For such a purpose, many different control strategies can be used. First, proportional-integral (PI) based control schemes were proposed to deal with the problem of maximum power point tracking [5], [6]. The authors presented control methods using the conventional and direct-current vector configuration to implement the maximum power extraction. It should be realized that PI control is a linear regulator, which is suitable for linear time invariant systems. However, the electrical and mechanical components in wind turbines work globally as nonlinear systems where electromechanical parameters vary considerably. Additionally, wind turbines are expected to operate effectively under a wide range of wind speeds; therefore, control designs become more complicated. To overcome this drawback, there are many different intelligent and nonlinear control strategies, such as gain scheduling [7], fuzzy logic control [8], neural network [9], feedback linearization [10], and backstepping [11]. In this context, methods based on sliding mode control (SMC) seem to be an

Manuscript received Jan. 7, 2015; accepted Apr. 24, 2015
Recommended for publication by Associate Editor Kyo-Beum Lee.
[†]Corresponding Author: phandinhhieucdt@gmail.com
Tel: +86-155-731-40966, Hunan University
[*]Faculty of Mechanical Engineering, Hanoi University of Industry, Vietnam
[**]College of Electrical and Information Engineering, Hunan University, Hunan, P.R. China

interesting approach because they make plants more robust and invariant with respect to matched uncertainties and disturbance. Concerning these methods, SMC schemes have been proposed in many studies [12]-[15]. The authors proposed one of these control strategies applied to the field-oriented control (FOC) to relatively overcome the effect of model uncertainties and wind speed turbulence [15]. However, its discontinuity of control variables results in variable switching frequency of the generator-side converter; thus, it may lead to a high chattering phenomenon and mechanical stress effect [13]. To keep a constant switching frequency without sacrificing robustness and tracking ability, second-order sliding mode control strategies were adopted [16]-[18]. Among them, the super-twisting algorithm (STA) has a simple law and allows synthesizing a continuous control action with discontinuous time derivative, which makes the trajectories reach the 2-sliding manifold in finite time and significantly reduces the chattering phenomenon. The disadvantage of the traditional STA is that it does not allow compensating uncertainties and turbulence growing together with the state variable; therefore, the sliding motion cannot be assured. To overcome this problem, the STA with variable gains (VGSTA) was proposed [19]. The proposed algorithm, whose adaptive gains are determined by the known functions, allows the exact compensation of smooth uncertainties and turbulence bounded together with their derivative by the known function. The new advanced algorithm was presented in literature [20], [21] where a VGSTA controller was developed for a WECS double output induction generator (WECS-DOIG), and this controller was applied to the WECS doubly fed induction generator (WECS - DFIG). To develop the new advanced algorithm for the multiple input multiple output (MIMO) of the WECS–PMSG, a VGSTA controller was designed in this paper. Using the Lyapunov function, the convergence of state variables was proved and the convergence time was estimated. In this paper, the results of the simulation demonstrated a better VGSTA control quality compared with the fixed-gain variable STA. This controller is not difficult to implement; thus, the computational burden is low during the online operation of the controller.

II. Wind Turbine System Description

Wind energy first transformed into mechanical energy through the wind turbine blades and then into electrical energy through the PMSG. The PMSG is connected into the grid through a two-level back-to-back converter. The electrical power is completely delivered to the grid by regulating the controller of the two-level back-to-back converter, which consists of a machine side converter (MSC), a grid side converter (GSC), and a DC link. The generator side control comprising the current control loop and speed control loop is presented in Fig. 1.

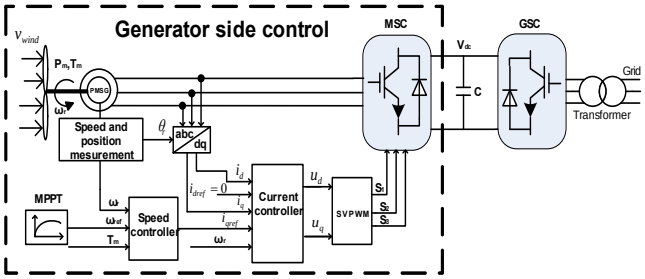

Fig. 1. Control block diagram of the PMSG.

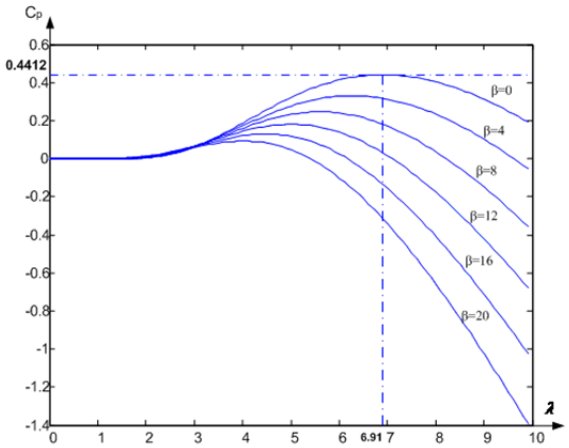

Fig. 2. Power coefficient versus tip speed ratio. Optimum value $C_{p\max} = 0.4412$; $\lambda_{opt} = 6.91$

A. Wind Turbine Modeling

Aerodynamic power extracted from the wind is expressed by the following equation [8]:

$$P_m = 0.5\rho\pi\gamma^2 C_p(\lambda,\beta)v^3 \tag{1}$$

where ρ is the air density, γ is the wind turbine rotor radius, ν is the wind speed, and $C_p(\lambda,\beta)$ is the turbine power coefficient. This coefficient can be calculated as follows:

$$C_p(\lambda,\beta) = 0.73\left(\frac{151}{\lambda i} - 0.58\beta - 0.002\beta^{2.14} - 13.2\right)e^{\frac{-18.4}{\lambda_i}} \tag{2}$$

$$\lambda_i = \frac{1}{\frac{1}{\lambda + 0.002\beta} - \frac{0.003}{\beta^3 + 1}}$$

where β is the blade pitch angle, and λ is the tip speed ratio, which is defined as [10]:

$$\lambda = \frac{\gamma w_r}{v} \tag{3}$$

where w_r is the angular speed of the rotor.

To effectively extract wind power while maintaining safe operation, the wind turbine should operate in two possible regions, namely, high and low speed regions [16]. In the high-speed region, the wind turbine must limit the captured wind power so that it does not exceed the rated power of the PMSG to maintain the safety of the electrical and mechanical loads. Control of the blade pitch is typically used to limit the power and speed wind turbine in this region. Meanwhile,

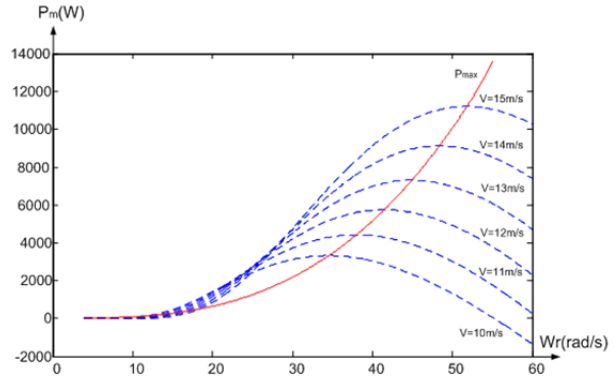

Fig. 3. Turbine characteristic with maximum power point tracking.

control of speed, torque, and power is frequently implemented in the low speed region to extract the maximum power from the wind. In this paper, speed control is used in the low speed region to reach maximum power extraction without controlling pitch blade angle ($\beta = const$).

From Equ. (2), the $C_p - \lambda$ characteristics, for different values of the pitch angle β, are shown in Fig. 2. From Fig. 2, the wind turbine operates with a constant pitch angle $\beta = 0^o$ and the maximum power coefficient $C_{p\max} = 0.4412$ is achieved for an optimum tip speed ratio value $\lambda_{opt} = 6.91$. Thus, the reference rotor speed of wind turbine is given by:

$$w_{ref} = \frac{v\lambda_{opt}}{\gamma} \tag{4}$$

The $P_m - w_r$ characteristics with maximum power point tracking for variable wind speed are presented in Figure 3, which shows that for any wind speed value, there is a unique rotor speed that generates the maximum power $P_{\max}$.

From Equ. (1), Equ. (3), and Equ. (4), the maximum mechanical power is written as follows:

$$P_{\max} = \frac{0.5\rho\pi\gamma^5 C_{p\max}}{\lambda_{opt}^3} w_r^3 = K_{opt} w_r^3 \tag{5}$$

Aerodynamic torque can be expressed as [15]:

$$T_{\max} = \frac{P_{\max}}{w_r} = K_{opt} w_r^2 \tag{6}$$

B. PMSG Modeling

Dynamic modeling of the PMSG can be described in (d,q) synchronous rotating reference frame, and is given by the following equations [22]:

$$U_d = R_s i_d + L_s \frac{di_d}{dt} - L_s p w_r i_q \tag{7}$$

$$U_q = R_s i_q + L_s \frac{di_q}{dt} + L_s p w_r i_d + p w_r \Psi_r \tag{8}$$

where i_d, i_q are the d-axis and q-axis stator current, respectively, U_d and U_q are the d-axis and q-axis stator voltage, respectively, R_s is the resistance of stator windings, L_s is the inductance of stator windings, Ψ_r is the permanent magnetic flux, and p is the number of pole pairs of the PMSG.

Moreover, the electromagnetic torque of the PMSG is computed using the following equation:

$$T_e = \frac{3}{2} p \Psi_r i_q = K_t i_q \tag{9}$$

with $K_t = \frac{3}{2} p \Psi_r$. Finally, the dynamic equation of the wind turbine is expressed as follows:

$$J \frac{dw_r}{dt} = T_m - T_e - \kappa w_r \tag{10}$$

where J represents the inertia of the rotating parts, κ is the viscous friction coefficient, and T_m denotes the aerodynamic torque.

From Equs. (7)–(10), the dynamic characteristics of the PMSG modeling with variation of parameters can be expressed as follows [15], [23]:

$$U_d = (L_{sn} + \Delta L_s)\frac{di_d}{dt} + (R_{sn} + \Delta R_s) i_d - (L_{sn} + \Delta L_s) p w_r i_q \tag{11}$$

$$U_q = (L_{sn} + \Delta L_s)\frac{di_q}{dt} + (R_{sn} + \Delta R_s) i_q + (L_{sn} + \Delta L_s) p w_r i_d + p w_r (\Psi_{rn} + \Delta\Psi_r) \tag{12}$$

$$T_m = (J_n + \Delta J)\frac{dw_r}{dt} + (\kappa_n + \Delta\kappa) w_r + (K_{tn} + \Delta K_t) i_q \tag{13}$$

where $L_{sn}, R_{sn}, \Psi_{rn}, J_n, \kappa_n, K_{tn}$ are the nominal values; $\Delta R_s, \Delta L_s, \Delta\Psi_r, \Delta\kappa, \Delta K_t$ represent the variations of parameters. These variations of parameters are assumed less than 50% of the nominal parameters. Then, the PMSG modeling can be rewritten as:

$$\frac{di_d}{dt} = \underbrace{\left(-\frac{R_{sn}}{L_{sn}} i_d + p w_r i_q\right)}_{f_1} + \underbrace{\left(\frac{-\Delta R_s}{L_{sn}} i_d - \frac{\Delta L_s}{L_{sn}}\frac{di_d}{dt} + \frac{\Delta L_s}{L_{sn}} p w_r i_q\right)}_{\Delta f_1} + \underbrace{\frac{1}{L_{sn}} U_d}_{u_1} \tag{14}$$

$$\frac{di_q}{dt} = \underbrace{\left(-\frac{R_{sn}}{L_{sn}} i_q - p w_r i_d - \frac{p w_r}{L_{sn}} \Psi_{rn}\right)}_{f_2} + \underbrace{\left(\frac{-\Delta R_s}{L_{sn}} i_q - \frac{\Delta L_s}{L_{sn}}\frac{di_q}{dt} - \frac{\Delta L_s}{L_{sn}} p w_r i_d - \frac{p w_r}{L_{sn}} \Delta\Psi_{rn}\right)}_{\Delta f_2} + \underbrace{\frac{1}{L_{sn}} U_q}_{u_2} \tag{15}$$

$$\frac{dw_r}{dt} = \underbrace{\left(-\frac{\kappa_n}{J_n} w_r + \frac{1}{J_n} T_m\right)}_{f_3} + \underbrace{\left(\frac{-\Delta J_n}{J_n}\frac{dw_r}{dt} - \frac{\Delta\kappa}{J_n} w_r - \frac{\Delta K_t}{J_n} i_q\right)}_{\Delta f_3} - \underbrace{\frac{K_{tn}}{J_n} i_q}_{u_3} \tag{16}$$

where the functions f_1, f_2, and f_3 represent the nominal model. Meanwhile, the functions $\Delta f_1, \Delta f_2, \Delta f_3$ denote the modeling errors and parameter uncertainties, and the signals u_1, u_2, u_3 are the control input variables.

III. CONTROL SYSTEM

A. Control Design

At this point, to achieve the desired control objectives when operating in the sliding mode, the sliding variables can be chosen as:

$$\begin{aligned} s_1 &= i_d - i_{dref} \\ s_2 &= i_q - i_{qref} \\ s_3 &= w_r - w_{ref} \end{aligned} \tag{17}$$

where i_{dref} and i_{qref} are the reference values of the stator current, w_{ref} denotes the reference value of rotor speed of the PMSG. Taking the time derivative of the sliding variables Equ. (17), incorporated with Equs. (14)–(16), leads to:

$$\begin{aligned} \dot{s}_1 &= \dot{i}_d - \dot{i}_{dref} = -\dot{i}_{dref} + f_1 + \Delta f_1 + u_1 \\ \dot{s}_2 &= \dot{i}_q - \dot{i}_{qref} = -\dot{i}_{qref} + f_2 + \Delta f_2 + u_2 \\ \dot{s}_3 &= \dot{w}_r - \dot{w}_{ref} = -\dot{w}_{ref} + f_3 + \Delta f_3 + u_3 \end{aligned} \tag{18}$$

Moreover, each component of the action control variables consist of two terms [21]:

$$u_i = u_{eqi} + \tilde{u}_i \tag{19}$$

where u_{eqi} (i=1,2,3) are the equivalent control terms for the nominal and unperturbed model, and $\tilde{u}_i$ is the term of control variables designed by using the STA with variable gains [19]. The expression for the equivalent control term u_{eqi} can be determined as [21]:

$$\begin{aligned} u_{eq1} &= i_{dref} - f_1 \\ u_{eq2} &= i_{qref} - f_2 \\ u_{eq3} &= w_{ref} - f_3 \end{aligned} \tag{20}$$

Substituting Equ. (20) and Equ. (19) into Equ. (18) produces:

$$\dot{s}_i = \tilde{u}_i + \Delta f_i \tag{21}$$

Functions Δf_i are divided into two terms expressed as:

$$\Delta f_i = g_{1i}(s,t) + g_{2i}(t) \tag{22}$$

where the functions $g_{1i}(s,t) = 0$ when $s_i = 0$, and the functions $g_{2i}(t)$ are the perturbations on the 2-SM manifold.

By contrast, the components of the control term $\tilde{u}_i$ can be given as [21]:

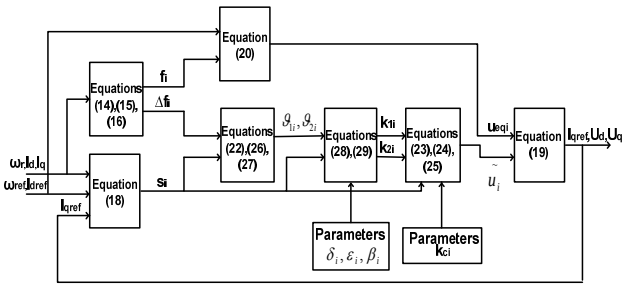

Fig. 4. Block diagram of the controller.

$$\tilde{u}_i = -k_{1i}(s,t)\phi_{1i}(s_i) - \int_0^t k_{2i}(s,t)\phi_{2i}(s_i)dt \tag{23}$$

$$\phi_{1i}(s_i) = k_{ci}|s_i|^{1/2} sign(s_i) \tag{24}$$

$$\phi_{2i}(s_i) = \frac{k_{ci}^2}{2} sign(s_i) = \phi_{1i}^{'}(s_i)\phi_{1i}(s_i) \tag{25}$$

where $\phi_{1i}^{'}(s_i) = \frac{k_{ci}}{2} s_i^{-1/2}$ is the partial derivative of $\phi_{1i}(s_i)$ with respect to s_i, and k_{ci} >0 is the constant. Values $k_{1i}(s,t)$ and $k_{2i}(s,t)$ are the variable gains which are determined by certain bounding functions of Equ. (26), Equ. (27). Then, the functions $g_{1i}(s,t)$ and the time derivative the functions $g_{12}(s,t)$ are bounded by the following equations:

$$|g_{1i}(s,t)| \le \vartheta_{1i}(s,t)|\phi_{1i}(s_i)| \tag{26}$$

$$\left|\frac{dg_{2i}(s,t)}{dt}\right| \le \vartheta_{2i}(s,t)|\phi_{2i}(s_i)| \tag{27}$$

where $\vartheta_{1i}(s,t)$ and $\vartheta_{2i}(s,t)$ denote the known positive functions. Under these conditions, the finite-time convergence to the 2-SM manifold and the robustness against all disturbance and uncertainty considered in functions Δf_i are guaranteed if the variable gains of Equ. (23) are calculated as:

$$\begin{aligned} k_{1i}(s,t) = \delta_i + \frac{1}{\beta_i}[(2\varepsilon_i\vartheta_{1i} + \vartheta_{2i})^2/(4\varepsilon_i) + \varepsilon_i + 2\varepsilon_i\vartheta_{2i} + \\ (2\varepsilon_i + \vartheta_{1i})(\beta_i + 4\varepsilon_i^2)] \end{aligned} \tag{28}$$

$$k_{2i}(s,t) = \beta_i + 4\varepsilon_i^2 + \varepsilon_i k_{1i} \tag{29}$$

where β_i, ε_i, and δ_i are the arbitrary constants.

A block diagram of the controller is presented in Fig. 4.

B. Stability of Control System

Defining $z_i = -\int_0^t k_{2i}(s,t)\phi_{2i}(s_i)dt + g_{2i}(t)$ as new states. The closed loop system for Equ. (21) with the VGSTA control law of Equ. (23) can be written as follows:

$$\dot{s}_i = -k_{1i}(s,t)\phi_{1i}(s_i) + z_i + g_{1i}(s,t) \tag{30}$$

$$\dot{z}_i = -k_{2i}(s,t)\phi_{2i}(s_i) + \frac{dg_{2i}(s,t)}{dt} \tag{31}$$

The Lyapunov function can be chosen as:

$$V = \sum_{1}^{3} V_i = \sum_{1}^{3} \varsigma_i^T P_i \varsigma_i = \varsigma_1^T P_1 \varsigma_1 + \varsigma_2^T P_2 \varsigma_2 + \varsigma_3^T P_3 \varsigma_3 \quad (32)$$

where $\varsigma_i^T = [\phi_{1i}(s_i), z_i]$ and $P_i = P_i^T = \begin{bmatrix} \beta_i + 4\varepsilon_i^2 & -2\varepsilon_i \\ -2\varepsilon_i & 0 \end{bmatrix} > 0$

The time derivative of each term V_i can be calculated as [21]:

$$\dot{V}_i = -\phi_{1i}^{'}(s_i)\varsigma_i^T Q_i \varsigma_i \quad (33)$$

where $Q_i = [A_i^T P_i + P_i A_i]$

$$A_i = \begin{bmatrix} k_{1i}(s,t) - \alpha_{1i}(s,t) & 1 \\ k_{2i}(s,t) - \alpha_{2i}(s,t) & 0 \end{bmatrix}$$

The values $\alpha_{1i}(s,t)$ and $\alpha_{2i}(s,t)$ are derived from the equations:

$$g_{1i} = \alpha_{1i}(s,t)\phi_{1i}(s_i)$$
$$\frac{dg_{2i}}{dt} = \alpha_{2i}(s,t)\phi_{2i}(s_i) \quad (34)$$

From [19], the built matrix $[Q_i - 2\varepsilon_i I]$ is positive definite, where I is the identity matrix of size 2. Thus, Equ. (33) can be bounded as follows:

$$\dot{V}_i \le -2\varepsilon_i \phi_{1i}^{'}(s_i)\varsigma_i^T \varsigma_i = -2\varepsilon_i \phi_{1i}^{'} \|\varsigma_i\|_2^2 = -\varepsilon_i k_{ci} |s_i|^{-1/2} \|\varsigma_i\|_2^2 \quad (35)$$

where $\|\varsigma_i\|_2^2$ represents the square of the 2-Euclidean norm determined as:

$$\|\varsigma_i\|_2^2 = \phi_{1i}^2 + z_i^2 = k_{ci}^2 |s_i| + z_i^2 \quad (36)$$

Additionally, the standard inequality for quadratic forms:

$$\lambda_m(P_i)\|\varsigma_i\|_2^2 \le V_i = \varsigma_i^T P_i \varsigma_i \le \lambda_M(P_i)\|\varsigma_i\|_2^2 \quad (37)$$

where $\lambda_m(P_i)$, $\lambda_M(P_i)$ are the minimum and maximum eigenvalues of matrix P_i, respectively. From Equ. (36) and Equ. (37), the following inequalities can be expressed as:

$$V_i^{1/2} \ge \lambda_m^{1/2}(P_i)\|\varsigma_i\|_2 \ge \lambda_m^{1/2}(P_i) k_{ci} |s_i|^{1/2} \quad (38)$$

$$\|\varsigma_i\|_2^2 \ge \frac{V_i}{\lambda_M(P_i)} \quad (39)$$

From Equ. (35), Equ. (38), and Equ. (39), the time derivative of V_i can be bounded as:

$$\dot{V}_i \le \frac{-\varepsilon_i k_{ci}^2 \lambda_m^{1/2}(P_i)}{\lambda_M^{1/2}(P_i)} V_i^{1/2} = -h_i V_i^{1/2} \quad (40)$$

where $h_i = \frac{\varepsilon_i k_{ci}^2 \lambda_m^{1/2}(P_i)}{\lambda_M^{1/2}(P_i)} > 0$, which shows that the V function is a strong Lyapunov function. Finally, the total time derivative of V_i is bounded as follows:

$$\dot{V} = \sum_{1}^{3} \dot{V}_i \le \sum_{1}^{3} -h_i V_i < 0 \quad (41)$$

From Equ. (32), Equ. (41), V is positive definite and $\dot{V}$ is negative definite, by considering the principle [24], the trajectories of Equ. (30), Equ. (31) converge to zero in the finite time.

TABLE I
WIND TURBINE PARAMETER VALUES

Rotor radius	2 m
Air density	$1.2\,kg/m^3$
Rated wind speed	14 m/s
Maximum power coefficient	0.4412
Optimal tip speed ratio	6.91
Winding resistance	0.45 ohm
Winding inductance	0.835 mH
Flux linkage	0.69833 Wb
Pole pairs	2
Mechanical inertia	$0.15\,kgm^2$
Viscous friction	$0.01\,kgm^2/s$
PMSG wind turbine power	10 Kw

C. Fixed-Gains – STA

The fixed-gain STA is used to compare with VGSTA. In this case, the term $\tilde{u}_i$ in Equ. (21) is similar to Equ. (23), but using fixed-gains can be expressed as follows:

$$\tilde{u}_i = -k_{1i}\phi_{1i}(s_i) - k_{2i}\int_0^t \phi_{2i}(s_i)dt \quad (42)$$

$$\phi_{1i}(s_i) = |s_i|^{1/2} sign(s_i) \quad (43)$$

$$\phi_{2i}(s_i) = \frac{1}{2} sign(s_i) \quad (44)$$

where k_{1i}, k_{2i} are the fixed-gain. From Equ. (30), Equ. (31), the bounding the components of g_i is:

$$|g_{1i}(s_i,t)| \le \delta_{1i}|s_i|^{1/2} \quad (45)$$

$$\left|\frac{d}{dt} g_{2i}(t)\right| \le \delta_{2i} \quad (46)$$

where δ_{1i}, δ_{2i} are the positive constants, and the fixed-gain can be chosen as:

$$k_{1i} \ge 2\delta_{1i} \quad (47)$$

$$k_{2i} \ge k_{1i}\frac{5\delta_{1i} + 6\delta_{2i} + 4(\delta_{1i} + \delta_{2i}/k_{1i})^2}{2(k_{1i} - 2\delta_{1i})} \quad (\text{i} = 1, 2, 3)$$

IV. SIMULATION RESULT

To verify the validity of the proposed algorithm, Matlab–Simulink was performed for a 10 kW PMSG wind turbine system. The parameters of the wind turbine are listed in Table I. During the simulations, the discrete model was used with a simulation time step of 5 μs . The sample time of the proposed control was 50 μs , and switching frequency converters was set at 2.5 kHz. Of the variable parameters, 50% were considered for wind turbine system. Namely:

$\Delta R_s = 0.225, \Delta L_s = 0.0004175, \Delta\Psi_r = 0.349165, \Delta J = 0.075,$
$\Delta K = 0.005$

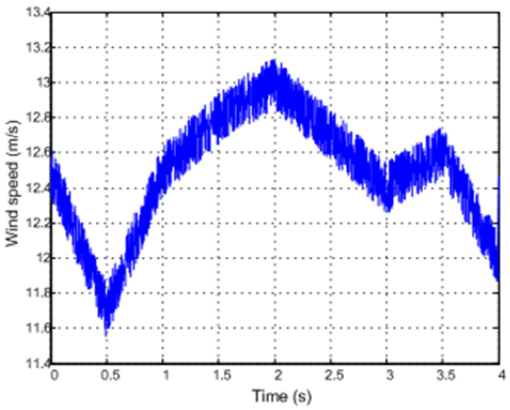

(a)

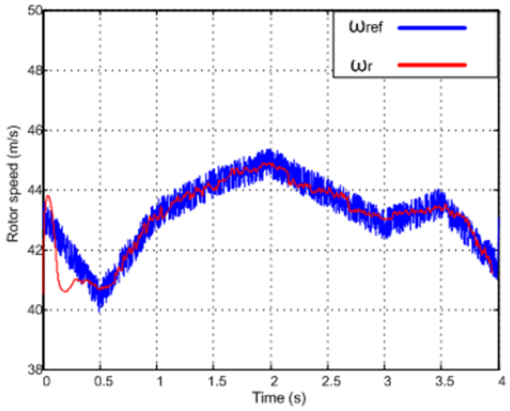

(b)

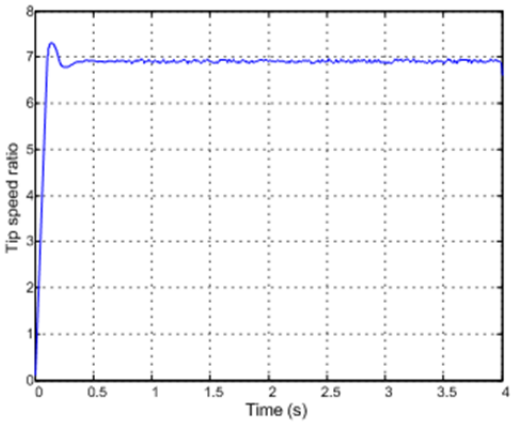

(c)

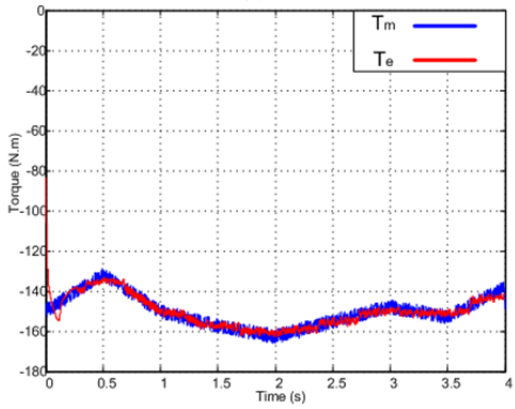

(d)

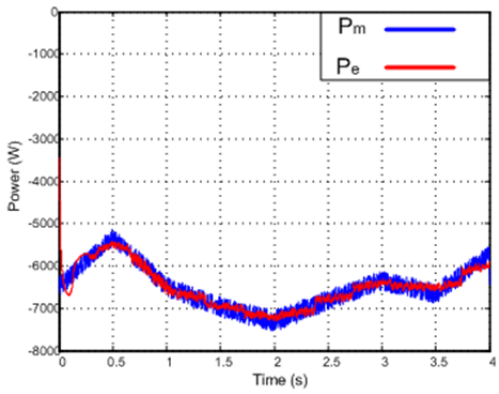

(e)

Fig. 5. (a) Wind velocity profile (m/s). (b) Rotor speed and rotor speed reference. (c) Tip speed ratio. (d) Aerodynamic torque and electromagnetic torque. (e) Mechanical power and generator active power.

Moreover, the following VGSTA controller settings were used:

$$\begin{aligned} &k_{c1}=20;\delta_1=10^{-4};\varepsilon_1=0.1;\beta_1=1;\\ &k_{c2}=40;\delta_2=10^{-4};\varepsilon_2=0.02;\beta_2=10;\\ &k_{c3}=20;\delta_3=10^{-4};\varepsilon_3=0.0025;\beta_3=100; \end{aligned} \tag{48}$$

For the STA controller, the fixed-gains can be chosen as follows:

$$\begin{aligned} &k_{11}=k_{12}=12.5; \quad k_{13}=67.75;\\ &k_{21}=k_{22}=76.3; \quad k_{23}=35.8; \end{aligned} \tag{49}$$

Fig. 5 shows the ability of tracking their reference value of the control variable in generator side control using the VGSTA controller for current control loop and speed control loop. The wind speed profile is shown in Fig. 5(a). Wind speed consists of the mean speed varying between 11 m/s and 13 m/s with the time interval [0, 4s] and the wind speed turbulence with 15% turbulence intensity. In response to the wind speed profile, the actual rotor speed (ω_r) and its reference value (ω_{ref}) are shown in Fig. 5(b). The rotor speed with the proposed controller tracks more closely the reference value, which is the optimal rotor speed leading to more power capture from nature wind. In Fig. 5(c), the tip speed ratio equals its optimum value ($\lambda_{opt}=6.91$) with a small oscillation ensuring the maximum power extraction.

Fig. 5(d) and Fig. 5(e) reveal that, despite the wind speed turbulence and variable parameters, the electromagnetic torque and active power of the PMSG accurately follow their reference values. The reference value P_m describes the maximum power extracted from the wind, and the reference value T_m denotes the aerodynamic torque calculated from the measurements. Although the chatter electromagnetic torque and the chatter active power exist because of the speed turbulence and the high converter frequency, it is a small value considered acceptable.

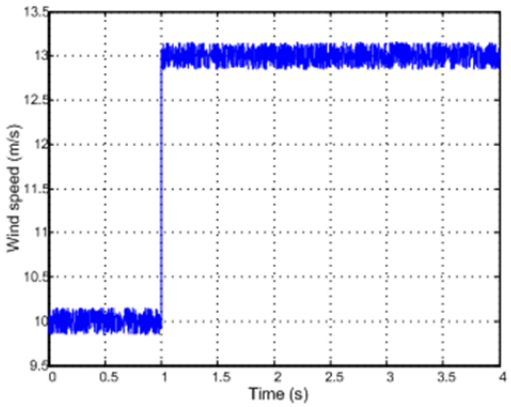

(a)

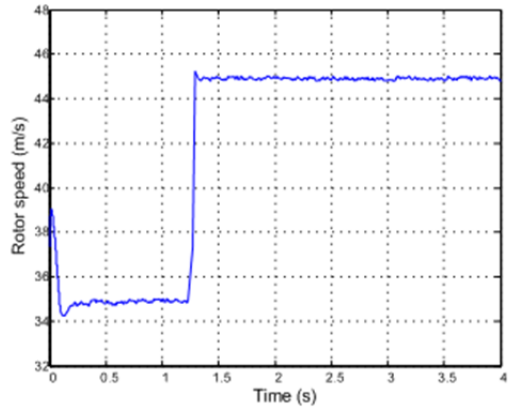

(b)

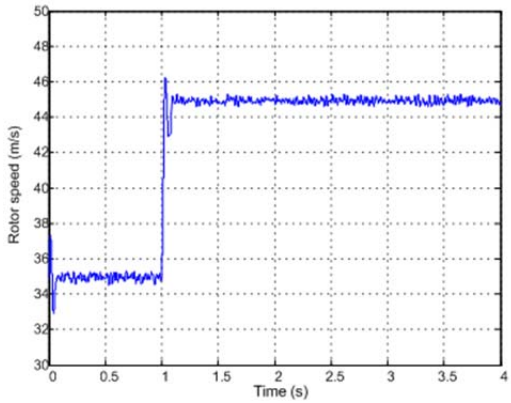

(c)

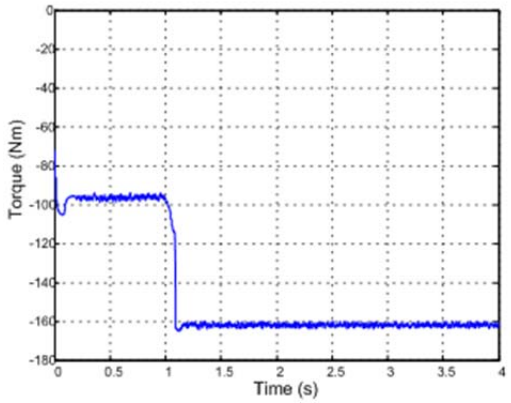

(d)

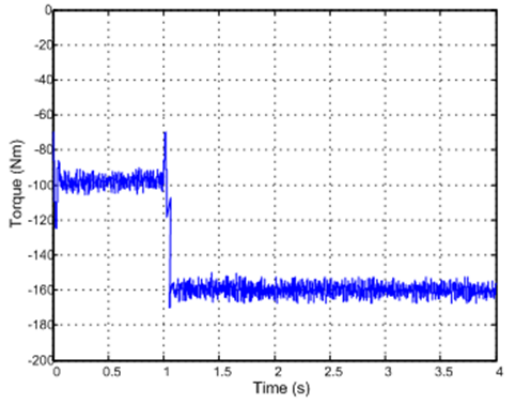

(e)

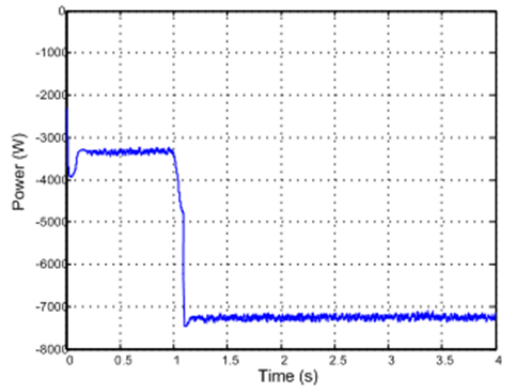

(f)

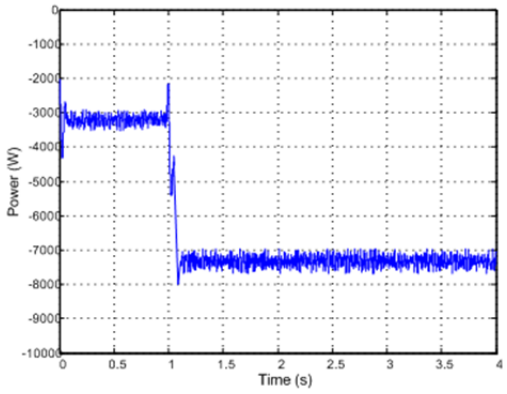

(g)

Fig. 6. (a) Wind speed profile (m/s). (b) Rotor wind speed (VGSTA). (c) Rotor wind speed (STA). (d) Electromagnetic torque (VGSTA). (e) Electromagnetic torque (STA). (f) Generator active power (VGSTA). (g) Generator active power (STA).

Fig. 6 shows the comparisons of the characteristics of the PMSG controlled by the VGSTA and STA under the aforementioned variable parameters. In these comparisons, the assumption is that the wind speed profile consists of the step value changing from 10 m/s to 13 m/s at 1 s and the turbulence shown in the Fig. 6(a). The rotor wind speed is governed by the VGSTA (see Fig. 6(b)) and the STA illustrated in Fig. 6(c). These figures reveal a smaller oscillation of the rotor wind speed regulated by the VGSTA against the one regulated by

the STA. Moreover, the comparisons of the electromagnetic torque are implemented in Fig. 6(d) (VGSTA) and Fig. 6(e) (STA). The chatter electromagnetic torque governed by VGSTA, kept below 2% its rated value, is much smaller than the one controlled by STA. A similar situation also happens in Fig. 6(f) and Fig. 6(g). VGSTA is much better than STA in this control system. The different comparison of the VGSTA and STA is derived from their control gains. The variable gains (VGSTA) allow compensating the uncertainties and the turbulences increasing in the system states, whereas the fixed-gains (STA) cannot do this. Thus, to maintain the robustness of the system under variable parameters and the wind turbulences, the fixed-gains (STA) must be much larger leading to the growth of the chatter signals in the wind system. Meanwhile, the VGSTA whose adaptive gains vary according to the system states completely reduces the chattering phenomenon affecting the system.

V. CONCLUSION

A cascaded control system of a wind turbine based on VGSTA was proposed for a variable speed wind energy conversion system. With controlled speed wind turbine under disturbance conditions, two main goals are achieved. First, generator side control ensures maximum power extraction regardless of wind speed turbulence and parameter variation. Second, it considerably reduces chatter active power and electromagnetic torque, avoiding the damage of excessive mechanical stress wind turbine. The candidate Lyapunov function was chosen for the cascaded control loops of the wind turbine system. By using this function, designing the control laws for cascaded control loops and demonstrating the convergence of the algorithm is easy. The most important contribution of this study is the successful application of this algorithm to control the current control loop and speed control loop, and the demonstration of the advantages of this algorithm over the traditional STA. The problem of VGSTA is that it is not simple to exactly determine the known bounded functions derived from the disturbances and to turn parameters of this controller. However, computational burden is low during the online operation of the controller. Finally, the excellent performances of VGSTA were verified by simulation results under wind speed noise and parameters derivation.

REFERENCES

[1] GWEC global wind energy council, *Global wind statistics 2013*, http://www.gwec.net, Feb. 2014.

[2] B. Wu, Y. Lang, N. Zargari, S. Kouro, *Power conversion and control of wind energy system*, John Wiley&Son, Chap.1, 2011.

[3] M. Chinchilla, S. Arnaltes, and J. C. Burgos, "Control of permanent magnet generators applied to variable-speed wind-energy systems connected to the grid," *IEEE Trans. Energy Convers.*, Vol. 21, No. 1, pp. 130-135, Mar. 2006.

[4] H. Polinder, F. F.Avan der Pijl, and P. Tavner, "Comparison of direct-drive and geared generator concepts for wind turbines," *IEEE Trans. Energy Convers.*, Vol. 21, No. 3, pp. 543-550, Sep. 2006.

[5] S. Li, T. A. Haskew, and L. Xu, "Conventional and novel control designs for direct driven PMSG wind turbines," *Electr. Power Syst. Res.*, Vol. 80, No. 3, pp. 328-338, Mar. 2010.

[6] S. Li, T. A. Haskew, R. P. Swatloski, and W. Gathings, "Optimal and direct-current vector control direct-driven PMSG wind turbines," *IEEE Trans. Power Electron.*, Vol. 27, No.5, pp. 2325-2337, May 2012.

[7] F. D. Bianchi, H. N. D. Battista, and R. J. Mantz, *Wind turbine control systems: Principles, Modeling and Gain Scheduling Design*, Springer-Verlag, Chap.6, 2007.

[8] S. M. Muyeen, and Ahmed Al – Durra, "Modeling and control strategies of fuzzy logic controlled inverter system for grid interconnected variable speed wind generator," *IEEE Syst. J.*, Vol.7, No. 4, pp. 817-824, Dec. 2013.

[9] E. Cadenas and W. Rivera, "Short term wind speed forecasting in La Venta, Oaxaca, Mexico, using artificial neural networks," *Renew. Energy*, Vol. 34, No. 1, pp. 274-278, Jan. 2009.

[10] K. H Kim, Y. C Jeung, D. C Lee, and H. G Kim, "LVRT scheme of PMSG wind power systems based on feedback linearization, " *IEEE Trans. Power Electron*., Vol. 27, No. 5, pp. 2376-2384, May 2012.

[11] A. El Magri, F. Giri, G. Besanc, A. E. Fadili, L. Dugard, and F. Z. Chaoui, "Sensorless adaptive output feedback control of wind energy systems with PMSG generators," *Control Eng. Pract*., Vol. 21, No. 4, pp. 530-543, Dec. 2012.

[12] B. Beltran, T. Ahmed-Ali, and M. E. H. Benbouzid, "Sliding mode power control of variable-speed wind energy conversion systems," *IEEE Trans. Energy Convers.*, Vol. 23, No. 2, pp. 551-558, Jun. 2008.

[13] M. I. Martinez, G. Tapia, A. Susperregui, and H. Camblong "Sliding-mode control for DFIG rotor and grid-side converters under unbalanced and harmonically distorted grid voltage," *IEEE Trans. Energy Convers*., Vol. 27, No.2, pp. 328-338, Jun. 2012.

[14] L. Shang and J. Hu, "Sliding-mode-based direct power control of grid-connected wind-turbine-driven doubly fed induction generators under unbalanced grid voltage conditions," *IEEE Trans. Energy Convers*., Vol.27, No. 2, pp. 362-373, Jun. 2012.

[15] M. L. Corradini, G. Ippoliti, and G. Orlando, "Robust control of variable-speed wind turbines based on an aerodynamic torque observer," *IEEE Trans. Contr. Syst. Technol.*, Vol. 27, No. 4, pp. 1199-1206, Jul. 2013.

[16] B. Beltran, T. Ahmed-Ali, and M. Benbouzid, "High-order sliding-mode control of variable-speed wind turbines," *IEEE Trans. Ind. Electron*., Vol. 56, No. 9, pp. 3314-3321, Sep. 2009.

[17] J. A. Moreno and M. Osorio, "A Lyapunov approach to second-order sliding mode controllers and observers," in *Proc. 47th IEEE Conf. Decis. Control*, pp. 2856-2861, 2008.

[18] S. Benelghali, M. E. H. Benbouzid, J. Charpentier, T. Ahmed-Ali, and I. Munteanu, "Experimental validation of a marine current turbine simulator: Application to a permanent magnet synchronous generator-based system second-order sliding mode control," *IEEE Trans. Ind. Electron.*, Vol. 58, No. 1, pp. 118-126, Jan. 2011.

[19] A. D´avila, J. Moreno, and L. Fridman, "Variable gains

Super-Twisting algorithm: A Lyapunov based design," *Amer. Control Conf.*, pp. 968-973, 2010.
[20] C. Evangelista, P. Puleston, F. Valenciaga, and L. Fridman, "Lyapunov designed Super-twisting sliding mode control for wind energy conversion optimization," *IEEE Trans. Ind. Electron.*, Vol. 60, No. 2, pp. 538-545, Feb. 2012.
[21] C. Evangelista, F. Valenciaga, and P. Puleston, "Active and reactive power control for wind turbine based on a MIMO 2-Sliding mode algorithm with variable gains," *IEEE Trans. Energy Convers.*, Vol.28, No. 3, pp. 682-689, Sep. 2013.
[22] S. Alepuz, A. Calle, S. B. Monge, S. Kouro, and B. Wu, "Use of stored energy in PMSG rotor inertia for low-voltage ride-through in back-to-back NPC converter-based wind power systems," *IEEE Trans. Ind. Electron.*, Vol. 60, No. 5, pp. 1787-1796, May. 2013.
[23] K. H. Kim and M. J. Youn, "A simple and robust digital current control technique of a PM synchronous motor using time delay control approach," *IEEE Trans. Power Electron.*, Vol. 16, No. 1, pp. 72-82, Jan. 2001.
[24] H. Khalil, *Nonlinear Systems*, NJ: Prentice-Hall, Chap.3 2002.

Dinh Hieu Phan was born in Vietnam in 1983. He received his B.S., M.S. in Automation Engineering from Hanoi University of Science and Technology, Hanoi, Vietnam, in 2006 and 2008, respectively. Since 2008, he has worked at the Mechatronics Department Mechanical Faculty of Hanoi University of Industry, as a Full Lecturer. He is currently working toward a Ph.D. degree at the College of Electrical and Information Engineering, Hunan University, China. His current research interests include electric machine control and control of distributed generation systems using renewable energy sources.

ShouDao Huang was born in China in 1962. He received a B.S. degree in Electric Machine and a Ph.D. degree in Electrical Engineering from Hunan University, China, in 1983 and 2000, respectively. From 1983 to 1993, he worked at the Hunan Motor factory as a technical Director. Since 1995, he has been with the College of Electrical and Information Engineering, Hunan University. From 2008 to 2009, he was a Visiting Scholar at the Energy College, Aalborg University, Denmark. He is currently a Vice President of the College of Electrical and Information Engineering, Hunan University. He is also an Executive Director of the Transactions of China Electrotechnical Society, a Director of the Hunan Association and Automation, a Director of the Energy Association of China, and a Committee Member of the large Motor Electrotechnical Society of China. His current research interests include power electronics and machine technology, control of power converters, wind power generation, and power quality.